Computational Development of a Dual Pre-Chamber Engine Concept for Lean Burn Combustion

2016-01-2242
Published 10/17/2016

Dimitris Assanis
University of Michigan

Nayan Engineer and Paul Neuman
Hyundai-Kia America Technical Center Inc

Margaret Wooldridge
University of Michigan

CITATION: Assanis, D., Engineer, N., Neuman, P., and Wooldridge, M., "Computational Development of a Dual Pre-Chamber Engine Concept for Lean Burn Combustion," SAE Technical Paper 2016-01-2242, 2016, doi:10.4271/2016-01-2242.

Abstract

Pre-chambers are a means to enable lean burn combustion strategies which can increase the thermal efficiency of gasoline spark ignition internal combustion engines. A new engine concept is evaluated in this work using computational simulations of non-reacting flow. The objective of the computational study was to evaluate the feasibility of several engine design configurations combined with fuel injection strategies to create local fuel/air mixtures in the pre-chambers above the ignition and flammability limits, while maintaining lean conditions in the main combustion chamber. The current work used computational fluid dynamics to develop a novel combustion chamber geometry where the flow was evaluated through a series of six design iterations to create ignitable mixtures (based on fuel-to-air equivalence ratio, ϕ) using fuel injection profiles and flow control via the piston, cylinder head, and pre-chamber geometry. The desirable and undesirable features that guided the design progression are presented. Major combustion chamber design iterations involved changes to the pre-chambers position relative to the cylinder head deck plane, azimuthal orientation of the pre-chambers, and piston crown geometry. Further criteria were developed to assess the flow interaction with the nozzle connections to the pre-chambers. The modeling results indicated appropriate fueling strategies achieved near stoichiometric fuel-to-air equivalence ratios in the pre-chambers with lean fuel-to-air equivalence ratios in the main chamber. The results also demonstrated the utility of the flow-alignment and chamber filling criteria to select the nozzle design for the pre-chambers.

Introduction

Lean burn combustion strategies are an attractive option to increase the thermal efficiency of gasoline spark ignition internal combustion engines, but engine design remains challenging due to the lean flammability limits of the fuel/air mixture. Lean aftertreatment strategies can be a concern; however, recent advances show considerable promise for effective emissions control for lean burn gasoline direct injection engines [1]. Turbulent jet ignition originating from a combustion pre-chamber can help address mixture flammability limits by ejecting high enthalpy and highly reactive jets into the main chamber, enabling lean combustion in the main chamber. However, appropriate mixture conditions must be achieved in the pre-chamber for this strategy to be successful.

Pre-chambers have been studied extensively in the past, in particular for application in compression ignition engines, and pre-chambers have been successfully demonstrated as technology which can improve in-cylinder combustion robustness [2, 3, 4]. Past learnings of pre-chamber technologies, including studies of the effects of heat transfer and mixture stratification, have guided the size, shape, orientation, and number of pre-chambers [5,6]. The engine concept proposed in this work is based on a new pre-chamber engine design where the spark electrodes are located in the pre-chamber and a direct injection (DI) fuel injector is located in the main chamber. Supplemental fueling (e.g. DI or port fuel injection (PFI)) is used to create the initial fuel/air charge in the main combustion chamber. To the best of our knowledge, this approach differs from any pre-chamber engine designs previously considered. The design was enabled by advances in numerical simulations, computational resources, fuel injection hardware, and manufacturing techniques. Specifically, the objective of the design process documented here was to develop a combustion system where lean fuel-to-air equivalence ratios are created in the main chamber while near stoichiometric equivalence ratios are created in the pre-chambers using the DI fuel injector.

Background

With the passing of the Clean Air Act of 1970 and the subsequent establishment of the Environmental Protection Agency, engine technologies offering significantly reduced tailpipe emissions started gaining major attention. Notably, gasoline pre-chamber engine

concepts offered a promising solution to decreasing mobile sources of air pollution by increasing fuel efficiency and by decreasing engine-out emissions [7]. Pre-chamber engine concepts are not a new technology to the automotive industry. H.R. Ricardo's internal combustion engine, documented in 1918, is the earliest pre-chamber concept found in the literature [8]. The pollution regulations of the 1970's brought renewed focus on the pre-chamber engine concept from research institutions and industry [9, 10, 11, 12, 13, 14, 15]. Most of the pre-chamber engine concepts suffered from atypical induction designs that required complicated valvetrain arrangements [9]; however, recent advances in numerical simulations and computational resources allowed gasoline pre-chamber engine concepts to be systematically considered in new configurations. The comprehensive review by Toulson et al. [6] outlined the progress of pre-chamber initiated combustion systems throughout history and provided sound engineering and scientific foundations for new engine designs which leveraged the best features of pre-chambers. Attard et al. [16] demonstrated an auxiliary-fueled turbulent jet ignition pre-chamber concept in a GM Ecotec engine platform capable of achieving 42% peak net indicated thermal efficiency without the need for a complicated valvetrain induction system. In comparison, the standard GM Ecotec engine platform achieved a peak net indicated thermal efficiency of 37.9% in stoichiometric spark ignition mode of operation.

The work presented in this paper focused on designing a prototype pre-chamber engine that reduces system complexity by eliminating the need for an auxiliary fuel injector located in the pre-chamber. Instead, the pre-chambers were designed to be fueled using an injection event from a fuel injector centrally mounted in the main combustion chamber (i.e. a gasoline DI system). This design concept leverages the advanced capabilities of modern fuel injectors and targets overall fuel lean operation. The technical approach used CFD to evaluate non-reacting in-cylinder flows of fuel and air achieved through different engine geometries. The designs were evaluated using metrics defined in the study to assess the efficacy of the flow at achieving the desired equivalence ratios in the pre-chambers and the main chamber.

Computational Methodology

The commercial software CONVERGE™ (versions 2.1.0-2.2.0) was used for the CFD study. The software platform was selected based on the adaptive mesh refinement capabilities. Matlab R2014a-R2014b was used to post-process the output files and derive flow metrics. Ensight 10.1 was used to visualize the output data. Relevant boundary conditions and initial conditions were derived from a validated GT-Power (v7.4) engine model for all cases.

The flow field in the three-dimensional, moving boundary domain was modelled as compressible, viscous and non-reactive and used a k-ε turbulence model and temperature law-of-the-wall boundary conditions. The pressure solver first used a point-wise successive over-relaxation algorithm before using an efficient geometric multigrid procedure. A finite volume numerical discretization scheme was used to solve momentum, energy and species equations. Pressure-velocity coupling was accomplished using the pressure-implicit-with-splitting-of-operators method in conjunction with the Rhie-Chow interpolation scheme.

Iso-octane, i-C_8H_{18}, was used as the fuel and air was 23% oxygen (mass basis) and 77% nitrogen for all simulations. Dilution of the fuel/air charge with exhaust gas residual species was not considered in these studies. The spray rate profile was modeled as a square step function with a targeted peak injection pressure of 149 ± 1 bar. The duration of the fuel injection event was varied to achieve the total mass of fuel desired. The fuel injector was represented as two identical nozzles 180° opposed in the azimuthal direction, each with a nozzle diameter of 150 µm, circular injection radius of 75 µm, and nozzle radial position of 1.5 mm.

The liquid fuel spray, injected at 335 K, was modeled using 50,000 parcels per injector based on a sensitivity study and best practices recommendations from the software manufacturer. The parcels were modeled as a bulk injection with the fuel droplet size distribution based on the nozzle size, and the parcels were distributed evenly throughout the spray cone [17]. Kelvin-Helmholtz (KH) and Rayleigh-Taylor (RT) models were used to represent the primary spray breakup. The secondary spray breakup was modeled using child parcels and by examining the competing effects of the KH and RT breakup models [18]. The specific model parameters used for the simulations are provided in the Supplementary Material and were based on the recommendations by CONVERGE for engine simulations of the type considered here. Further detail on the modeling parameters and theory can be found to in Senecal et al. [19] and Richards et al. [18].

The initial engine geometry for the new engine concept was based on a conventional inline four cylinder 2.0 L forced-induction gasoline production engine. The geometry of a single cylinder of the base engine is presented in Figure 1.

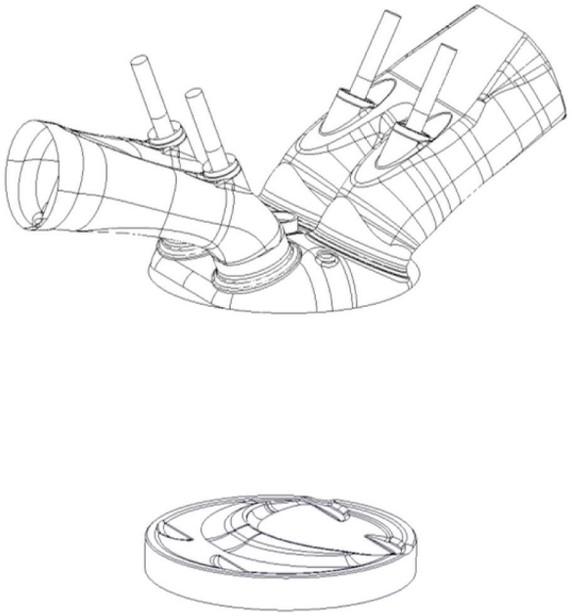

Figure 1. Production base geometry (bottom dead center position) used as the starting point for the engine design process.

The production engine featured a four-valve design, centrally-mounted spark plug, side-mounted direct injector, and a piston crown designed to enhance mixing. The geometric specifications of the base engine and the final engine design (designated the Zeta prototype) are presented in Table 1.

Initial intake and exhaust valve timings were taken from the production engine and modified to maximize volumetric efficiency within the constraints of the maximum allowable phasing of the production variable valve timing system. The intake valve phasing was ultimately limited by piston - valve interference, due to the geometry of the piston crown.

A total of 7 regions (defined by virtual boundaries in the simulation) were defined to develop flow metrics to evaluate the performance of the different engine designs. The boundaries, regions, associated initial conditions, and event timings are provided in the Supplementary Material. All calculations used initialization values for turbulent kinetic energy (TKE) of 1.0 m^2/s^2 and for TKE dissipation rate of 10 m^2/s^3. The computational mesh was a modified cut-cell Cartesian grid [18]. The base cell size for the entire engine geometry mesh was set as a 4 mm cubic cell. Both fixed embedding and adaptive mesh refinement were utilized to locally refine the base mesh and create efficient and accurate grids at each time step. Portions of the main combustion chamber and the pre-chambers were further refined between 1 and 0.5 mm cubic cells. The volume defined by the projected bore area extended 17 mm past the cylinder head deck plane into the cylinder head and was populated with 1 mm cubic cells to ensure a smooth continuation of the flow from the port to the main combustion chamber. The remaining volume defined by the projected bore area into the cylinder head was populated with 2 mm cubic cells to help transition the flow from the base 4 mm cubic mesh found in the ports.

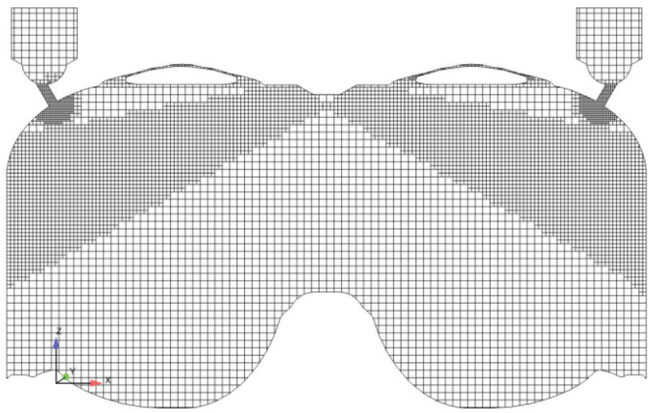

Figure 2. Example mesh highlighting the fixed cell embedding at the piston centerline for the final Zeta prototype just before the booster injection occurs at 60°bTDC.

Two layers of 0.5 mm cubic cells were embedded off the intake and exhaust valve angle boundaries to ensure the flow past the valves was accurately captured during the valve opening and closing events. The volume surrounding and including the fuel spray was refined to 0.5 mm cubic cells to ensure the spray region was sufficiently resolved. Figure 2 features a representative mesh of the final Zeta prototype just before an injection event is about to occur at 60° bTDC.

Table 1. Summary of the specifications of the initial and final engine designs.

Specification	Base Engine	Zeta Prototype
Bore	86.0 mm	86.0 mm
Stoke	86.0 mm	86.0 mm
Connecting Rod Length	149.25 mm	146.25 mm
Wrist Pin Offset	0.8 mm	0.8 mm
Compression Ratio	9.5	10.25
Intake Valve Diameter	32.7 mm	35.0 mm
Intake Valve Opening[a]		316 CAD
Intake Valve Closing[a]		582 CAD
Exhaust Valve Diameter	26.0 mm	29.0 mm
Exhaust Valve Opening[a]		164 CAD
Exhaust Valve Closing[a]		403 CAD

[a]Valve events are specified at 1 mm lift.

Velocity-based adaptive mesh refinement was used for the cylinder and intake system regions. A maximum allowable cell count of 1,000,000 cells could be achieved due to the adaptive mesh refinement. When the sub-grid velocity field exceeded 1.0 m/s, the affected cells and immediate neighbors were refined by reducing the cell size to 0.5 mm during the next time step. The total maximum cell count for the simulation results presented here was less than 990,000 cells, and the maximum cell count during the injection event was less than 725,000 cells. The cell counts were sufficient to obtain the desired sub-grid velocity field criterion of less than 1.0 m/s. The grid and refinement techniques are based on best practices recommendations [13-14] to ensure a sufficiently resolved grid for gasoline, direct-injection, non-reacting simulations.

Prototype Development

The objective of the computational study was to identify an engine design which could create local fuel/air mixtures in the pre-chambers above the ignition and flammability limits (i.e. with fuel-to-air equivalence ratios at near stoichiometric values, $\phi \sim 1.0$), while maintaining lean conditions in the main combustion chamber. Rapid compression facility studies by Assanis et al. serve as a guidance for the flammability limits of lean and dilute iso-octane air mixtures in a combustion chamber [20]. While spark plugs will be used to ignite the mixtures in the pre-chambers, spark plugs were not included in the simulations and all flow was non-reacting.

A series of six prototype iterations, visual representations provided in Figure 3, were considered to meet the project targets for fueling. The designs varied the in-cylinder flow, the placement of the pre-chambers, and the fueling strategy to meet the target equivalence ratios for the pre-chamber and the main combustion chamber. The naming convention was based on the generation of the design, e.g. Alpha, Beta, etc. ending with Zeta. A summary of the major design features for each iteration is presented in Table 2.

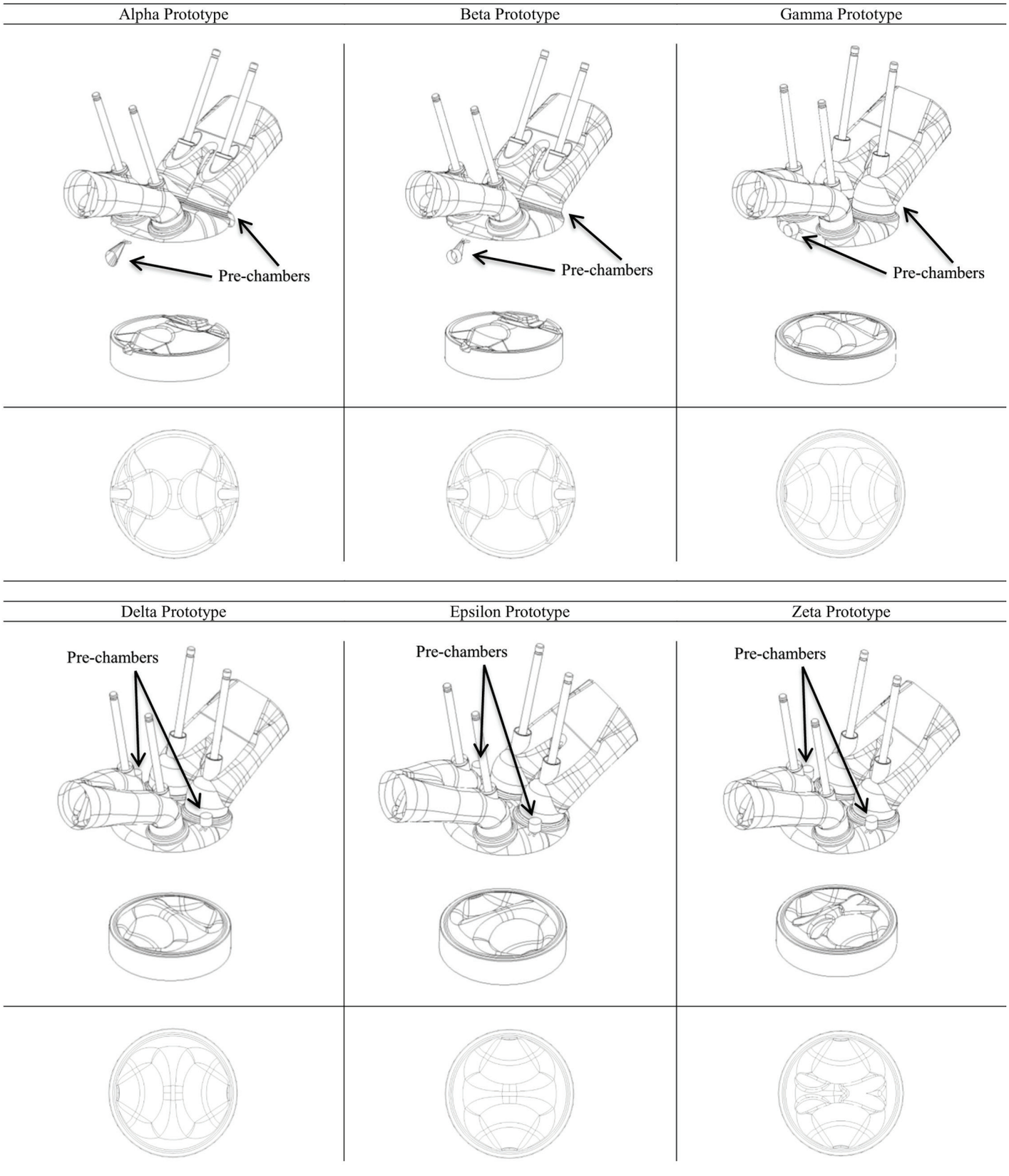

Figure 3. Visual representations of the prototype iterations (bottom dead center position) in each upper panel with top-view of the associated piston crown in each lower panel. The arrows indicate the locations of the pre-chambers.

The pre-chambers were designed to be indirectly fueled by a single injector located in the main combustion chamber. One end of each pre-chamber included the orifices to connect the pre-chamber to the main chamber. The number, size and orientation of the connecting orifices affect the pre-chamber filling process and were considered variable design parameters in this study. In an effort to simplify the pre-chamber design, no poppet valve assembly or auxiliary fuel injectors (features previously demonstrated in the literature, see [10]

and references therein) were located in the pre-chamber volume. Although spark plugs were not included in the simulation, packaging constraints of the pre-chambers were imposed to allow the pre-chamber spark plugs to be accessible for installation and maintenance. The pre-chambers were also located so they would not interfere with neighboring cylinders. Ease of manufacturing was also considered with the pre-chamber design.

The geometries of the piston crown, combustion chamber dome, and the intake port were designed to create favorable charge motion so a combustible mixture could be inducted into the pre-chambers by the time the piston reached the top dead center (TDC) position. The surface area to volume ratio of the pre-chamber geometry was selected to decrease heat transfer losses.

The production base engine geometry featured a centrally mounted spark-plug and a side-mounted injector. As noted earlier, the dual pre-chamber engine concept features a centrally mounted fuel injector in the main chamber with two opposed spray plumes targeted towards the pre-chambers. The central location of the fuel injector allowed for greater flexibility in creating a symmetric fuel spray pattern target flow to each of the pre-chambers.

The fueling amount used in the simulations was based on a typical engine operating condition of 2,000 RPM and 4 bar brake mean effective pressure (BMEP). This engine operating point required approximately 16 mg of fuel for typical SI operation. Since the dual pre-chamber engine concept targeted lean burn operation, the simulations considered 2 mg of fuel injected directly into the main combustion chamber by the direct injector. This fueling event is referred to as the booster injection, and is meant to create ignitable mixtures in the dual pre-chambers.

Table 2. Overview of key design features of the different prototype iterations and conclusions of initial computational simulations based on a 1 mg booster fuel injection event.

Prototype	**Key Design / Revision Features**	**Conclusions**
Alpha	• Orifices located in liner parallel to cylinder head deck. • Fuel spray was wall guided by the piston.	• Low pre-chamber equivalence ratio (ϕ ~ 0.15) • Poor pre-chamber fuel vapor fraction (~45% of the fuel mass in each pre-chamber) • Substantial main chamber wall film (70% of the total fuel mass) • Slight pre-chamber wall film (<5% of the total fuel mass)
Beta	• Central orifices widened and angled upwards to align with injector spray cone centerline. • Cut-out reliefs introduced in cylinder head dome to reduce wall wetting due to spray impingement.	• Higher pre-chamber equivalence ratio (ϕ ~ 0.6) • Poor pre-chamber vapor fraction (~45% of the fuel mass in each pre-chamber) • Minimal main chamber wall film (<0.5% of the total fuel mass) • Increased pre-chamber wall film (~23% of the fuel mass in each pre-chamber)
Gamma	• Pre-chambers relocated to the cylinder head under ports. • Combustion chamber dome re-designed. • Intake port re-designed for enhanced tumble. • Fuel spray now air guided by charge motion.	• Low pre-chamber equivalence ratio (ϕ ~ 0.1-0.2) • Excellent pre-chamber vapor fraction (100% of the fuel mass in each pre-chamber) • Slight main chamber wall film (<2% of the total fuel mass) • Pre-chamber wall film eliminated
Delta	• Pre-chambers rotated 90^{o} azimuthally about central Z-axis.	• Moderate pre-chamber equivalence ratio (ϕ ~ 0.3) • Excellent pre-chamber vapor fraction (100% of the fuel mass in each pre-chamber) • High main chamber wall film (<10% of the total fuel mass) • Pre-chamber wall film eliminated
Epsilon	• Piston rotated 90^{o} azimuthally about central Z-axis.	• Moderate pre-chamber equivalence ratio (ϕ ~ 0.3) • Excellent pre-chamber vapor fraction (100% of the fuel mass in each pre-chamber) • High main chamber wall film (<8% of the total fuel mass) • Pre-chamber wall film eliminated
Zeta	• New piston geometry with valve cut-outs for improved range of valvetrain phasing	• Moderate pre-chamber equivalence ratio (ϕ ~ 0.3) • Excellent pre-chamber vapor fraction (100% of the fuel mass in each pre-chamber) • Main chamber wall film eliminated • Pre-chamber wall film eliminated

In addition to the booster fuel injection event targeted for fueling the pre-chambers, a global injection event would be required in the engine to create the overall fuel lean charge in the main combustion chamber. This global injection event could be provided by the DI or a PFI injector. The global injection event would occur before the booster DI event, providing a background or baseline level of fuel in the main chamber. The booster injection would occur after the global injection event, late in the intake stroke, and would introduce a small amount of fuel targeted to create the near stoichiometric conditions in the pre-chambers. For this study, the global injection event was not included in the simulations, as it was assumed the global injection event would create a consistent background level of fuel in the main chamber and pre-chambers. This represents the most challenging situation for the booster injection, when there is no pre-existing background level of fuel in the main chamber or pre-chambers.

Results and Discussion

Prototype Performance

The major conclusions from the computational studies of the design prototypes are presented along with the major design features in Table 2. A key metric of prototype performance was the state of the fuel in the main chamber and pre-chambers. A summary of the fuel state from a booster injection event of 1 mg of fuel is presented by prototype iteration in Figure 4. The physical changes outlined in Table 2 were made to achieve fully vaporized fuel in the pre-chambers; a design feature which was met by the Zeta prototype.

Brief summaries of the design features of the prototypes are provided here. The Alpha prototype modified the production base geometry while attempting to integrate the pre-chambers as per the criteria described earlier. The intake port, exhaust port, and combustion chamber dome were unchanged. The two, diametrically opposed, pre-chambers were placed in the liner below the intake and exhaust ports. The pre-chambers were placed sufficiently below the cylinder head deck so the limiting dimension of the spark plug could clear the cylinder head gasket. Each conically shaped pre-chamber was sized as 1% of the total combustion chamber volume and included three horizontal connecting orifices, each with a nominal diameter of 1.25 mm. The pre-chamber volume sizing and orifice diameters were in alignment with recommendations set forth by Gussak et al. [21]. The Alpha prototype piston featured two scallops pointing towards each pre-chamber. When the piston was in the TDC position, the pre-chamber connecting orifices remained unobstructed. The Alpha prototype aimed to induct the charge mixture into the pre-chamber by transferring the charge mixture from the squish region through the connecting orifices to the pre-chamber.

For the Alpha prototype fueling strategy, two “pencil” sprays (i.e., with narrow spray cones), limited by the combustion chamber dome clearance, were aimed at a 125.5° included spray angle facing the narrow end of each scallop. One mg of fuel was injected at 149.5 bar rail pressure for a duration of 3.54 CAD. Spray patterns with included cone angles of 2.6° and 5° were simulated at the start of the injection (SOI) timings of 35° bTDC, 20° bTDC, and 5° bTDC. The most successful spray pattern, 5° cone angle and 20° bTDC SOI, resulted in only 6.6% of the total fuel vaporized in the two pre-chambers at TDC. In summary, the Alpha prototype with a 1 mg fuel injection was able to achieve $\phi = 0.15$ and $\phi = 0.13$ in pre-chamber A and B, respectively. The vaporized fuel fraction was 41% and 46% in pre-chambers A and B, respectively, with the remainder of the fuel fraction in the liquid phase in each pre-chamber.

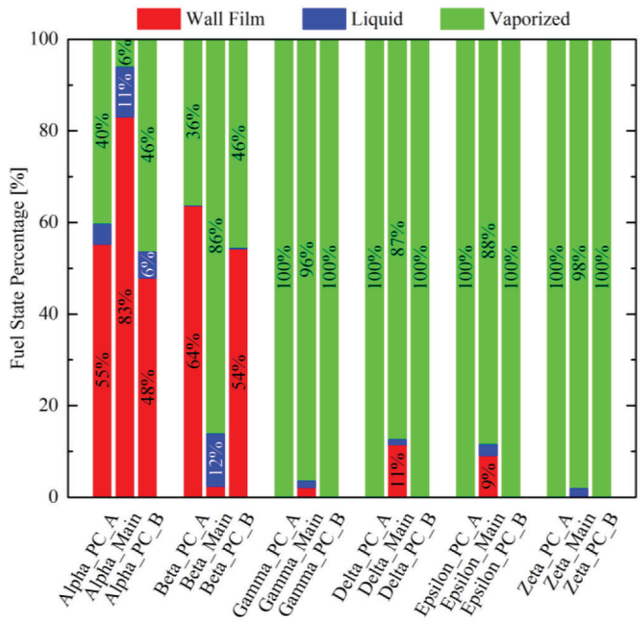

Figure 4. Summary of the fuel state (wall film, liquid, or vaporized) in the main chamber and pre-chambers by prototype iteration.

Using the most successful Alpha prototype spray profile, the mass of fuel injected was increased to 10 mg while keeping all other variables constant. The amount of vaporized fuel in the pre-chambers at TDC was approximately the same as for the 1 mg fuel injection at 6.2%. When the speed of the engine was doubled to 4000 RPM while setting the fueling amount at 1 mg, the amount of vaporized fuel in the pre-chambers at TDC decreased slightly to 6.0%.

The Beta prototype improved on the Alpha prototype by angling the central connecting orifice upwards to better match the fuel spray angle. The included spray angle for the two fuel jets was increased to 142.5° to directly target the central connecting orifice. The fueling amount was increased to 2 mg at the same rail pressure. Spray patterns with included cone angles of 2.6° and 5° were simulated at SOI timings of 60° bTDC, 40° bTDC, and 20° bTDC. The most successful spray pattern using 2 mg of fuel, a 5° cone angle and a 40° bTDC SOI, yielded ~50% of the total fuel as vapor in the two pre-chambers at TDC.

The Beta prototype with a 2 mg injection was able to achieve ϕ = 1.18 (with a vaporized fuel fraction of 50%) and ϕ = 1.24 (with a vaporized fuel fraction of 51%) in pre-chamber A and B, respectively. While the pre-chambers inducted enough fuel to achieve the design target of nearly stoichiometric mixtures, there was significant concern about the amount of liquid fuel present at TDC in each pre-chamber. 36.3% of the total fuel was predicted to result in wall films in the pre-chambers, occurring mostly in the connecting central orifice. The Beta design also raised concerns that the central orifice could clog during engine operation from fuel film effects such as coking or varnishing. The high levels of wall films could also be a source of unburned hydrocarbon and particulate emissions. The Gamma prototype aimed to improve the amount of vaporized fuel in the pre-chambers while simultaneously reducing the amount of liquid

fuel in the pre-chambers. The Gamma prototype avoided the use of the direct "pencil" type spray profile. Instead, the fuel spray was air-guided by rebounding the fuel off of a re-designed piston surface and into the pre-chambers which were re-located in the cylinder head. The approach allowed significantly longer mixing time, which increased vaporization of the fuel. To further enhance mixing and direct the fuel, the charge motion tumble was improved over the base production geometry by changing the intake valve angle and corresponding port design.

The new spray profile had the added benefit of eliminating the limitation of wetting the combustion chamber dome. So the included spray cone angle was increased to 20° to further assist fuel mixing. Sprays with included spray angles of 70°, 90°, and 140° were investigated at SOI of 40° bTDC. At 60° bTDC SOI, sprays with included spray angles of 40°, 80°, and 140° were evaluated. The velocity vector field was examined by creating various cut-planes along the cylinder. Comparing the velocity vectors of the cells along the two centerline cut-planes yielded interesting findings. The pre-chamber connecting orifices in the Gamma prototype were located in a region of significant recirculation. The charge mixture was circulated back towards the center of the combustion chamber instead of being inducted into the pre-chamber. Co-incidentally, 90º rotated in the azimuthal direction, the flow field was extremely favorable for re-locating the pre-chambers.

The Delta prototype featured the piston orientation of the Gamma prototype, but the pre-chambers were relocated 90º in the azimuthal direction in the cylinder head. The same parametric study of SOI and spray angle used to evaluate the Gamma prototype was applied to evaluate the Delta prototype. The highest amount of vaporized fuel in the two pre-chambers at TDC for the Delta prototype was associated with the 140° included spray angle and 60° bTDC SOI, and a 1 mg injection yielded $\phi = 0.29$ and $\phi = 0.30$ in pre-chambers A and B, respectively. The vaporized fuel fraction was 100% for both pre-chambers, a significant improvement over the Beta prototype.

The Epsilon prototype was identical to the Delta prototype, but the piston was rotated 90º in the azimuthal direction so the injection event could benefit from the proper orientation of the piston scallops. The intake and exhaust valve timings for the Epsilon prototype were identified using GT-Power to achieve the largest trapped air mass given the range of authority of the factory variable valve timing. The new piston orientation required the exhaust valve to be advanced by 10 CAD to prevent piston and valve interaction. The intake valve timing remained unchanged. The same parametric study of spray cone angle and SOI used for the Gamma and Delta designs was applied to the Epsilon prototype. The Epsilon prototype was able to induct a larger amount of charge mixture into the pre-chambers using the 20° and 40° included spray angles in comparison with the Delta prototype. These spray angles relied more significantly on the piston crown geometry to guide the charge mixture into the pre-chambers. The best fueling strategy for the Epsilon prototype occurred with the same SOI and same spray angle as the Delta prototype, and resulted in an approximately equal amount of charge mixture inducted in each pre-chamber. The tumble, caused by the valve angle and port geometry, was sufficiently intense that the tumble flow was the primary transport mechanism for the induction of the charge mixture into the pre-chambers at the included spray angle of 70º.

The Zeta prototype featured the same combustion chamber geometry as the Epsilon prototype, but the piston crown geometry was modified to avoid piston and valve interaction. A similar parametric study of spray cone angle, included spray angle, and SOI was conducted for the Zeta prototype. The spray pattern with the best results for the Zeta prototype was achieved with a 20° included spray cone angle and a 140° included spray angle. The results for the equivalence ratio at TDC in the pre-chambers and the main chamber for each of the prototype designs are compared in Table 3. The model predictions show the target goals of controlling the relative fuel quantities in the pre-chambers and the main chamber were met in the Delta, Epsilon and Zeta designs, and the Zeta design further achieved complete vaporization of the fuel in the pre-chamber with 98% vaporization in the main chamber.

The success of the Zeta prototype was due to the bulk charge motion developing a split reverse tumble motion. The intake port, combustion chamber dome, and piston geometry were designed to enable this motion. The fuel injected into the main chamber during the booster injection was successfully vaporized and transported towards and inducted into the pre-chambers. Figure 5 shows the velocity vector field of the Zeta prototype 1 mg fuel injection simulation on the centerline cut plane at 60° bTDC.

Table 3. Comparison of the model predictions for fuel mass and vapor fraction by region in the various prototypes at TDC for a 1 mg booster injection. The best results for pre-chamber equivalence ratio for the different spray cone angles and included spray angles considered are presented for each design.

Prototype	Start of Injection [°bTDC]	Main Chamber		Pre-Chamber A		Pre-Chamber B	
		ϕ	Vapor Fraction	ϕ	Vapor Fraction	ϕ	Vapor Fraction
Alpha	20°	0.00	6%	0.15	41%	0.13	46%
Beta	40°	0.01	81%	0.61	45%	0.63	46%
Gamma	60°	0.04	96%	0.09	100%	0.19	100%
Delta	60°	0.04	87%	0.29	100%	0.30	100%
Epsilon	60°	0.04	88%	0.29	100%	0.28	100%
Zeta	60°	0.06	98%	0.27	100%	0.29	100%

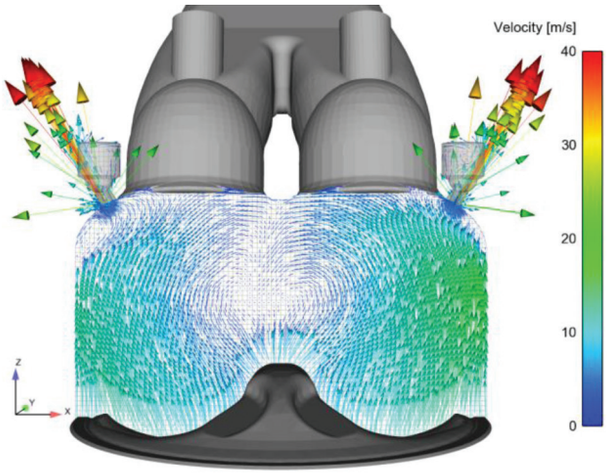

Figure 5. Velocity vector field at the centerline cut plane of the Zeta prototype at 70° bTDC highlighting the split reverse tumble motion of the bulk flow field for 1 mg of fuel injected at SOI = 60° bTDC.

Based on the positive results for the Zeta model predictions for fuel distribution and phase, a larger parametric space for fuel mass was explored for the Zeta prototype using a 20° spray cone angle and a 140° included spray angle, with fueling amounts from 1 mg to 7 mg and SOIs of 50º, 60º and 70º. Table 4 summarizes the results for fuel mass by region. The SOI of 60° bTDC yielded the best results in terms of equivalence ratios of vaporized fuel in the pre-chambers and the main chamber. Figure 6 presents the equivalence ratio in the pre-chambers and the main chamber for SOI of 60° bTDC as a function of the booster fuel mass injected. The pre-chambers achieved near stoichiometric mixtures of fully vaporized fuel with the 7 mg booster injection. The results also show the main chamber was fuel lean throughout the range of fuel mass considered.

Figure 6 and Table 4 show the amount of fuel injected in the booster event can be lower than 7 mg and achieve $\phi > 0.8$ conditions in the pre-chambers. The results indicate when the booster fueling event is superimposed on the conditions created by a global fuel injection event, near stoichiometric conditions can be achieved in the pre-chambers.

The results of the computational simulations were also interrogated to understand the transient behavior of the flow into and out of the pre-chambers. Using the flow field near the pre-chamber orifices, a flow field alignment metric was developed with the form:

$$Vel_{ratio} = \frac{\hat{V}_{zone} \cdot \hat{n}_{orifice}}{|\hat{V}_{zone}|} \quad (1)$$

where $\hat{V}_{zone}$ is the average velocity vector in a spherical region outside the pre-chamber orifices and in the main chamber, and $\hat{n}_{orifice}$ is the vector normal to the planar area of the opening of each orifice, with the positive direction chosen as towards the pre-chamber. The dot product of $\hat{V}_{zone}$ and $\hat{n}_{orifice}$ gives an absolute measure of how well the flow field is aligned with the orifice orientation.

Normalizing Vel_{ratio} by the magnitude of $\hat{V}_{zone}$ enables direct comparison between different flow conditions and engine designs. In this form, Vel_{ratio} quantifies the contribution of the local flow to filling and emptying the pre-chamber, where Vel_{ratio} can have a value between -1 and 1. A Vel_{ratio} value of 0 indicates the local flow is bypassing the connecting orifice. A Vel_{ratio} value of +1 indicates the local flow is perfectly aligned and filling the pre-chamber. A Vel_{ratio} value of -1 indicates the flow is perfectly aligned and emptying the pre-chamber.

Table 4. Summary of model predictions for fuel mass and vapor fraction by region in the Zeta prototype at TDC for an included spray cone angle of 20° and an included spray angle of 140°.

	Start of	Main Chamber		Pre-Chamber A		Pre-Chamber B	
Fueling Amount	Injection [°bTDC]	ϕ	Vapor Fraction	ϕ	Vapor Fraction	ϕ	Vapor Fraction
1 mg	60°	0.06	98%	0.28	100%	0.27	100%
2 mg	60°	0.11	98%	0.48	100%	0.47	100%
3 mg	50°	0.17	95%	0.52	100%	0.52	100%
3 mg	60°	0.17	97%	0.62	100%	0.62	100%
3 mg	70°	0.17	98%	0.61	100%	0.59	100%
4 mg	50°	0.22	94%	0.61	100%	0.60	100%
4 mg	60°	0.22	95%	0.74	100%	0.74	100%
4 mg	70°	0.23	98%	0.72	100%	0.71	100%
5 mg	60°	0.28	93%	0.78	100%	0.83	100%
6 mg	60°	0.33	91%	0.90	100%	0.91	100%
7 mg	60°	0.38	90%	0.97	100%	0.97	100%

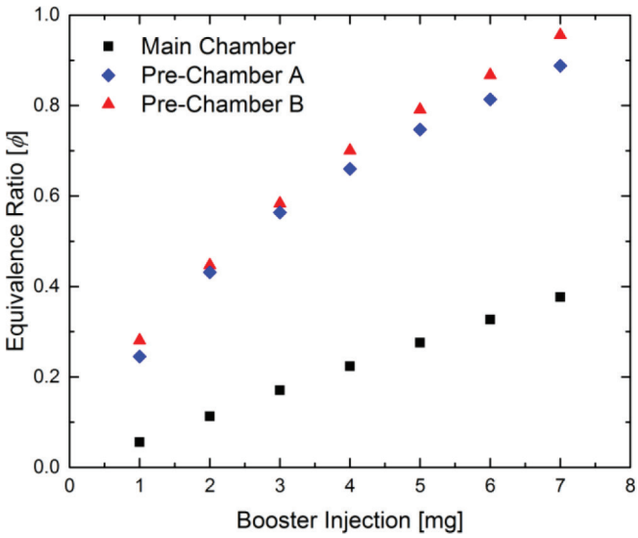

Figure 6. Equivalence ratio by region as a function of the fuel mass in the booster injection event for 20° included spray cone angle, 140° included spray angle, and SOI of 60° bTDC.

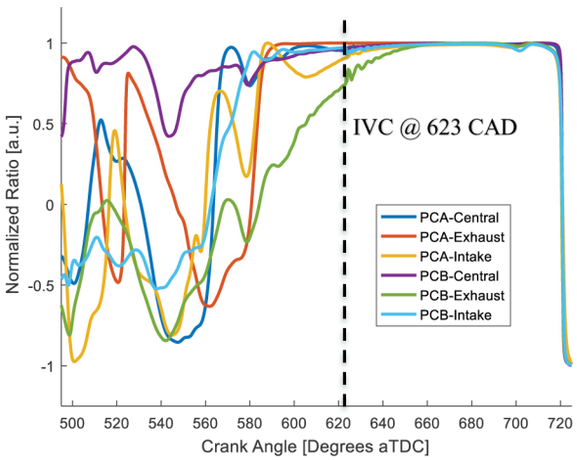

Figure 7. Vel_{ratio} for the pre-chamber orifices of the Beta prototype for a non-spraying simulation.

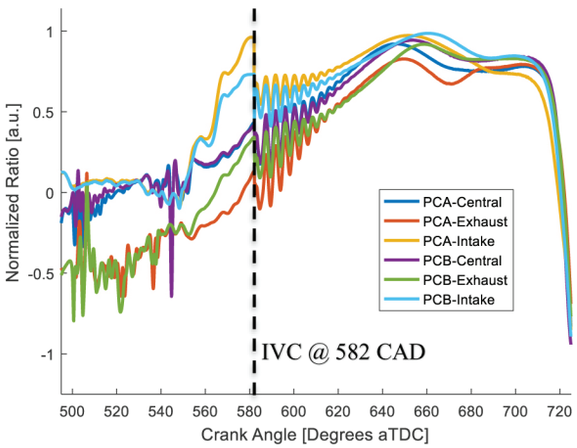

Figure 8. Vel_{ratio} for the pre-chamber orifices of the Zeta prototype for a non-spraying simulation.

Figures 7 and 8 present the results for Vel_{ratio} for the Beta and Zeta prototypes, respectively. The Beta and Zeta simulations were selected to highlight key features of the transient flow behavior. In the figures, the time histories for Vel_{ratio} for each of the six orifices are presented. The three orifices for each of the two pre-chambers are designated by their location relative to the exhaust valves, intake valves, and the central position.

Both prototype engine designs showed the full range of potential values for Vel_{ratio} from -1 to +1. When the piston changed directions, either at BDC (540 CAD) or TDC (720 CAD), the Vel_{ratio} captured the expected change in flow direction. Both engine designs showed the pre-chambers should be well-purged during the expansion stroke. The Beta prototype had an intake valve closing event, IVC, at 623 CAD, while the Zeta prototype had an intake valve closing event at 582 CAD. Both engine designs showed flow sensitivity immediately following IVC; however, the Zeta flow was more sensitive, with larger oscillations in Vel_{ratio} over a longer portion of the cycle. The lower sensitivity of the Beta design was due to the local flow being "saturated" in the alignment with the orifices, with $Vel_{ratio} \cong 1$, for a majority of the time between IVC and TDC. Recall the Beta design targeted direct filling of the pre-chambers by the booster fuel spray, and the direct alignment of the liquid fuel spray led to unacceptably high liquid films in the pre-chamber.

When comparing the values for Vel_{ratio} for the different orifices for the Zeta predictions in Figure 7, there is a period of time before the intake valve closes (~560 CAD to 580 CAD) where the orifices on the exhaust side of the chamber had flow exiting the pre-chambers while flow through the other orifices were filling the pre-chambers. This may lead to short-circuiting of the flow, and this type of behavior can be a constraint on the timing of the booster fuel injection event. However, this type of behavior can also be desirable for purging the residuals from the pre-chambers depending on the timing. Similar simultaneous inflow and outflow behavior, although more erratic, was observed for the Beta model predictions before IVC. Note the decaying oscillations observed after IVC in the Zeta prototype results are likely due to the rapid numerical separation of the intake port and the combustion chamber and are likely an artifact of the solver. All convergence criteria are satisfied through this portion of the cycle. Soon after IVC, all orifices exhibited filling behavior for the Zeta model predictions (and the Beta model predictions). This portion of the cycle is when the booster fuel injection event occurred. A significant window of time when the flow is well-aligned with filling the pre-chambers is critical during this portion of the cycle to enable flexibility in the timing of the booster fuel injection event.

The intake and exhaust orifices for each pre-chamber were at significantly different angles for the Zeta prototype, yet Figure 8 shows the Vel_{ratio} values were comparable to the values for the central orifice. In other words, the flow alignment metric results for the Zeta prototype indicate little sensitivity of the flow to the angle of the pre-chamber orifices. This allows flexibility in strategically targeting the exhaust orifices of each pre-chamber to enable the shortest and most complete main chamber burn possible.

Summary and Conclusions

This work documented the development and evaluation of a new engine concept using computational simulations of non-reacting flow. The objective of the computational study was to evaluate the feasibility of several engine design configurations combined with fuel

injection strategies to create local fuel/air mixtures in the pre-chambers above the ignition and flammability limits, while maintaining lean conditions in the main combustion chamber.

Through a series of six design iterations, the Zeta prototype was able to achieve the desired ignitable mixture in the pre-chamber at TDC by using an appropriate fuel injection profile and flow control via the piston, cylinder head, and pre-chamber geometry. The ignitable mixture was achieved using an injection strategy of 7 mg of fuel at 60°bTDC SOI with a spray pattern featuring a 20° included spray cone angle and a 140° included spray angle. Each pre-chamber was able to achieve $\phi = 0.97$, which was near the nominal design target, while maintain a sufficiently lean global equivalence ratio of $\phi = 0.38$ in the main chamber. The fuel was fully vaporized in the pre-chambers and was 90% vaporized in the main chamber. This was achieved by the two, diametrically opposed, pre-chambers being indirectly fueled from a centrally mounted fuel injector in the main chamber and using the bulk charge motion to improve fuel spray mixing. The results of this design study show difficulties associated with pre-chamber charge preparation of indirectly fueled pre-chamber engine designs can be overcome.

Additionally, a flow field alignment metric was developed based on the flow field near the pre-chamber orifices. The metric quantified the contribution of the local flow to the filling and emptying of the pre-chamber and aided in understanding of the transient nature of the pre-chamber filling dynamics. Regardless of combustion chamber geometry, number of orifices, or pre-chamber location, the optimal injection strategy will be one that introduces the appropriate amount of vaporized fuel near the pre-chamber orifices at a span of time where the near orifice flow field is at the highest alignment with the normal vector of the orifice opening.

Current work focuses on building, characterizing and testing of the Zeta prototype via an optically accessible single cylinder engine. Experimental studies are in progress to validate the CFD model predictions and to further develop this lean burn combustion engine concept.

References

1. Philipp, S., Hoyer, R., Adam, F., Eckhoff, S. et al., "Exhaust Gas Aftertreatment for Lean Gasoline Direct Injection Engines - Potential for Future Applications," SAE Technical Paper 2013-01-1299, 2013, doi:10.4271/2013-01-1299.
2. Takashima, Y., Tanaka, H., Sako, T., and Furutani, M., "Evaluation of Engine Performance and Combustion in Natural Gas Engine with Pre-Chamber Plug under Lean Burn Conditions," *SAE Int. J. Engines* 8(1):221-229, 2015, doi:10.4271/2014-32-0103.
3. Shah, A., Tunestal, P., and Johansson, B., "Effect of Pre-Chamber Volume and Nozzle Diameter on Pre-Chamber Ignition in Heavy Duty Natural Gas Engines," SAE Technical Paper 2015-01-0867, 2015, doi:10.4271/2015-01-0867.
4. Szwaja, S., Jamrozik, A., and Tutak, W., "A two-stage combustion system for burning lean gasoline mixtures in a stationary spark ignited engine," *Appl. Energy* 105(x):271-281, 2013, doi:10.1016/j.apenergy.2012.12.080.
5. Watson, N. and Kamel, M., "Thermodynamic Efficiency Evaluation of an Indirect Injection Diesel Engine," SAE Technical Paper 790039, 1979, doi:10.4271/790039.
6. Toulson, E., Schock, H., and Attard, W., "A Review of Pre-Chamber Initiated Jet Ignition Combustion Systems," SAE Technical Paper 2010-01-2263, 2010, doi:10.4271/2010-01-2263.
7. Mavinahally, N.S., Assanis, D.N., Govinda Mallan, K.R., and Gopalakrishnan, K. V., "Torch Ignition: Ideal for Lean Burn Premixed-Charge Engines," *J. Eng. Gas Turbines Power* 116(October 1994):793, 1994, doi:10.1115/1.2906887.
8. Ricardo, H.R., "Internal Combustion Engine," U.S. Patent 1,271,942, United States, 1918.
9. Turkish, M., "3 - Valve Stratified Charge Engines: Evolvement, Analysis and Progression," SAE Technical Paper 741163, 1974, doi:10.4271/741163.
10. Purins, E., "Pre-Chamber Stratified Charge Engine Combustion Studies," SAE Technical Paper 741159, 1974, doi:10.4271/741159.
11. Varde, K.S., "An Optical Investigation of the Combustion of a ' Stratified Mixture in a Dual Chamber Confinement," 5(1):426-431, 1974.
12. Pischinger, F. and Klöcker, K., "Single-Cylinder Study of Stratified Charge Process with Prechamber-Injection," SAE Technical Paper 741162, 1974, doi:10.4271/741162.
13. Davis, G., Krieger, R., and Tabaczynski, R., "Analysis of the Flow and Combustion Processes of a Three-Valve Stratified Charge Engine with a Small Prechamber," SAE Technical Paper 741170, 1974, doi:10.4271/741170.
14. Brandstetter, W., Decker, G., Schafer, H., and Steinke, D., "The Volkswagen PCI Stratified Charge Concept-Results from the 1.6 Liter Air Cooled Engine," SAE Technical Paper 741173, 1974, doi:10.4271/741173.
15. Varde, K. and Lubin, M., "The Roll of Connecting Nozzle and the Flame Initiation Point in the Performance of a Dual Chamber Stratified Charge Engine," SAE Technical Paper 741161, 1974, doi:10.4271/741161.
16. Attard, W., Kohn, J., and Parsons, P., "Ignition Energy Development for a Spark Initiated Combustion System Capable of High Load, High Efficiency and Near Zero NOx Emissions," *SAE Int. J. Engines* 3(2):481-496, 2010, doi:10.4271/2010-32-0088.
17. Reitz, R. and Diwakar, R., "Structure of High-Pressure Fuel Sprays," SAE Technical Paper 870598, 1987, doi:10.4271/870598.
18. Richards, K.J., Senecal, P.K., and Pomraning, E., "CONVERGE (v2.2) Theory Manual," Madison, WI, 2015.
19. Senecal, P., Richards, K., Pomraning, E., Yang, T. et al., "A New Parallel Cut-Cell Cartesian CFD Code for Rapid Grid Generation Applied to In-Cylinder Diesel Engine Simulations," SAE Technical Paper 2007-01-0159, 2007, doi:10.4271/2007-01-0159.
20. Assanis, D., Wagnon, S.W., and Wooldridge, M.S., "An experimental study of flame and autoignition interactions of iso-octane and air mixtures," *Combust. Flame* 162(4):1214-1224, 2015, doi:10.1016/j.combustflame.2014.10.012.

21. Gussak, L., Turkish, M., and Siegla, D., "High Chemical Activity of Incomplete Combustion Products and a Method of Prechamber Torch Ignition for Avalanche Activation of Combustion in Internal Combustion Engines," SAE Technical Paper 750890, 1975, doi:10.4271/750890.

Contact Information

Author for correspondence:

Dimitris Assanis
dassanis@umich.edu
Department of Mechanical Engineering
The University of Michigan
Ann Arbor, MI, 48109, USA

Acknowledgements

The authors would like to thank the generous support of Convergent Science Inc. for granting an academic license and providing technical support when necessary. This research was supported in part through computational resources and services provided by Advanced Research Computing at the University of Michigan, Ann Arbor.

Definitions/Abbreviations

BDC - Bottom Dead Center

bTDC - before Top Dead Center

CFD - Computational Fluid Dynamics

DI - Direct Injection

KH - Kevin Helmholtz

PFI - Port Fuel Injection

RPM - Revolutions Per Minute

RT - Rayleigh Taylor

SOI - Start Of Injection

TDC - Top Dead Center

Symbols

γ - Ratio of Specific Heats

ε - Turbulent Dissipation

κ - Turbulent Kinetic Energy

ϕ - Equivalence Ratio

° - Degrees

Supplementary Material

Table A-1. Summary of the boundaries in the dual pre-chamber computational model.

ID	Name	Region Name	Boundary Type	Temperature [K]	Pressure [Pa]
1	Piston	Cylinder	Translating Wall	530	-
2	Liner	Cylinder	Stationary Wall	420	-
3	Head	Cylinder	Stationary Wall	435	-
4	Pre-Chamber A	Pre-Chamber A	Stationary Wall	400	-
5	Orifices A	Orifices A	Stationary Wall	500	
6	Pre-Chamber B	Pre-Chamber B	Stationary Wall	400	
7	Orifices B	Orifices B	Stationary Wall	500	
8	Intake Port	Intake System	Stationary Wall	400	-
9	Intake Valve Top	Intake System	Translating Wall	500	-
10	Intake Valve Angle	Intake System	Translating Wall	625	-
11	Intake Valve Bottom	Cylinder	Translating Wall	625	-
12	Exhaust Port	Exhaust System	Stationary Wall	450	-
13	Exhaust Valve Top	Exhaust System	Translating Wall	550	-
14	Exhaust Valve Angle	Exhaust System	Translating Wall	675	-
15	Exhaust Valve Bottom	Cylinder	Translating Wall	675	-
16	Inflow	Intake System	Inflow	Specified Profile	Specified Profile
17	Outflow	Exhaust System	Outflow	Specified Profile	Specified Profile

Table A-2. Summary of initial conditions for the regions in the dual pre-chamber computational model.

ID	Name	Temperature [K]	Pressure [kPa]
0	Cylinder	894	107.5
1	Intake System	320	61.8
2	Exhaust System	894	107.5
3	Pre-Chamber A	600	107.5
4	Pre-Chamber B	600	107.5
5	Orifices A	600	107.5
6	Orifices B	600	107.5

Table A-3. Summary of region event schedule for the dual pre-chamber computational model.

Event Type	Event Start [CAD]	Region 1	Region 2	Event
Cyclic	358	Cylinder	Intake System	Open
Cyclic	623	Cylinder	Intake System	Close
Cyclic	165	Cylinder	Exhaust System	Open
Cyclic	404	Cylinder	Exhaust System	Close
Permanent	-	Cylinder	Pre-Chamber A	Open
Permanent	-	Cylinder	Pre-Chamber B	Open
Permanent	-	Orifices A	Pre-Chamber A	Open
Permanent	-	Orifices B	Pre-Chamber B	Open

The Engineering Meetings Board has approved this paper for publication. It has successfully completed SAE's peer review process under the supervision of the session organizer. The process requires a minimum of three (3) reviews by industry experts.

ISSN 0148-7191

http://papers.sae.org/2016-01-2242